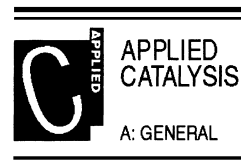




ELSEVIER

Applied Catalysis A: General 182 (1999) 327–336



# Selective *N*-monomethylation of aniline over $Zn_{1-x}Ni_xFe_2O_4$ ( $x=0, 0.2, 0.5, 0.8$ and 1) type systems

K. Sreekumar<sup>a</sup>, T. Raja<sup>b</sup>, B.P. Kiran<sup>b</sup>, S. Sugunan<sup>a</sup>, B.S. Rao<sup>a,b,\*</sup>

<sup>a</sup>Department of Applied Chemistry, Cochin University of Science and Technology, Cochin 682 022, India

<sup>b</sup>Catalysis Division, National Chemical Laboratory, Pune 411 008, India

Received 2 September 1998; received in revised form 2 December 1998; accepted 21 January 1999

## Abstract

The reaction of aniline with methanol was carried out over  $Zn_{1-x}Ni_xFe_2O_4$  ( $x=0, 0.2, 0.5, 0.8$  and 1) type systems in a fixed-bed down-flow reactor. It was observed that systems possessing low “ $x$ ” values are highly selective and active for mono *N*-alkylation of aniline leading to *N*-methyl aniline. Selectivity for *N*-methyl aniline over  $ZnFe_2O_4$  was more than 99% under the optimized reaction conditions. Even at methanol to aniline molar ratio of 2, the yield of *N*-methyl aniline was nearly 55.5%, whereas its yield exceeded 67% at the molar ratio of 7. The Lewis acid sites of the catalysts are mainly responsible for the good catalytic performance. Cation distribution in the spinel lattice influences their acido-basic properties, and hence, these factors have been considered as helpful to evaluate the activity and stability of the systems. © 1999 Elsevier Science B.V. All rights reserved.

**Keywords:** Ferrites; Spinel systems; Aniline conversion; *N*-Alkylation

## 1. Introduction

Ferros spinels, which form an important class of compounds having the general formula  $M^{II}[Fe^{III}Fe^{III}]O_4$ , find wide applications in both the technological and the catalytic field [1–5]. Their peculiar type of cation distribution among the tetrahedral (T) and octahedral (O) sites of the coordinated oxygen is an important factor in explaining the catalytic effectiveness. Based on the distribution of cations, spinels can be either normal  $M_{tet}^{2+}[Fe^{3+}Fe^{3+}]_{oct}O_4$  or inverse with half of the trivalent ions in the T-position and the other half together with the divalent ions in the O-sites.

Crystal field stabilization energy, Madelung constant and cation size are the principal factors in deciding the structure of the systems [6,7]. This peculiar structural feature enables spinels to withstand even extremely reducing conditions. Even if reduction of  $Fe^{3+}$  to  $Fe^{2+}$  occurs, the lattice configuration remains unaltered, and upon reoxidation, the original state can be regained. Several authors have reported that the major influence in the activity comes from the O-ions, probably due to the large exposure of these ions on the surface, as revealed by Jacobs et al. [8] using LEIS measurements (Low energy ion scattering, a technique which is sensitive to the outermost atomic layer). In the present series of compounds, all except  $ZnFe_2O_4$  are inverse in nature.  $Ni^{2+}$  replaces  $Fe^{3+}$  from the O-sites progressively as “ $x$ ” increases. In  $NiFe_2O_4$  ( $x=1$ )

\*Corresponding author. Fax: +91-212-33-4761; e-mail: bsrao@dalton.ncl.res.in

all  $\text{Ni}^{2+}$  and half of  $\text{Fe}^{3+}$  ions lie in the O-sites, whereas the other half of the  $\text{Fe}^{3+}$  ions lie in the T-sites. This type of cation distribution significantly affects their acido-basic properties. The present work is carried out with an objective of evaluating the catalytic activity of the systems in aniline alkylation as a function of composition and the subsequent variation in acidity and basicity. Cyclohexanol dehydration studies have been carried out to evaluate the acidity of the systems, whereas the limiting amount of electron acceptors like TCNQ and chloranil adsorbed have been taken as the measure of the basicity.

Alkylation of aniline is industrially important owing to the numerous uses of various substituted anilines like *N*-methyl aniline, *N,N*-dimethyl aniline and toluidines [9,10]. These are important raw materials for various agrochemicals, dyes, pharmaceuticals and explosives. A broad range of solid acid systems have been studied, due to their eco-friendly nature and their potential to replace the conventional Friedel–Crafts type systems [11–20]. Though metal oxides were reported to show better selectivity for *N*-alkylation over *C*-alkylation, usually many such systems afford both mono and disubstitution on nitrogen, leading to poor selectivity for the synthetically more important mono substituted product. Interestingly, our systems, particularly  $\text{ZnFe}_2\text{O}_4$  and  $\text{Zn}_{0.8}\text{Ni}_{0.2}\text{Fe}_2\text{O}_4$  were found to be highly selective for mono *N*-methylation of aniline, using methanol as the alkylating agent. High *N*-methyl aniline yield was observed even at comparatively low methanol to aniline molar ratio; this yield was significantly improved at high methanol to aniline molar ratio. An important observation was that, the increase in methanol concentration does not enhance *N,N*-dimethyl aniline yield significantly, high selectivity for *N*-methyl aniline was observed even at large methanol to aniline molar ratio. The amount of *C*-alkylated product was negligible in all the systems studied.

## 2. Experimental

### 2.1. Synthesis

The five compositions of the Zn–Ni ferrites viz.  $\text{ZnFe}_2\text{O}_4$  (ZF-1),  $\text{Zn}_{0.8}\text{Ni}_{0.2}\text{Fe}_2\text{O}_4$  (ZNF-2),  $\text{Zn}_{0.5}\text{Ni}_{0.5}\text{Fe}_2\text{O}_4$  (ZNF-3),  $\text{Zn}_{0.2}\text{Ni}_{0.8}\text{Fe}_2\text{O}_4$  (ZNF-4) and

$\text{NiFe}_2\text{O}_4$  (NF-5) were synthesized according to a published procedure [21]. The materials were powdered and calcined at  $300^\circ\text{C}$  for 36 h. Catalyst pellets of the required mesh size were then obtained by pressing under 10 t of pressure.

Unlike the spinels synthesized by the solid state high temperature methods, which produce systems with some inherent drawbacks like poor compositional control, chemical inhomogeneity and low surface area, this method provides chemically homogeneous and fine ferrite particles.

### 2.2. Characterization

#### 2.2.1. Structural analysis

The purity of the samples was first ensured by XRD (Rigaku, model D/MAX-VC) with  $\text{Cu K}\alpha$  radiation. All peaks in the pattern matched well with the characteristic reflections of Ni–Zn ferrite reported in the ASTM card No. 3-0875. The X-ray diffractogram of ZF-1 is presented in Fig. 1. Thermal stability of the samples was established by TG-DTA analysis on an automatic derivatograph (SETARAM-TG-DTA-92) using finely powdered  $\alpha$ -alumina as a reference material. Scanning electron micrographs showed fine grains of uniform size  $\approx 50$  nm, which was very much less than the grains of the spinels prepared by the conventional high temperature methods. All compositions of the systems showed two strong IR bands,  $\nu_1$  and  $\nu_2$ , around  $700$  and  $500\text{ cm}^{-1}$ , respectively (Fig. 2). It was systematically assigned by Waldren

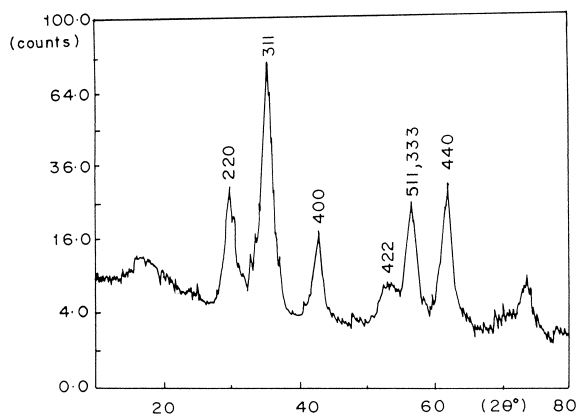


Fig. 1. X-ray diffractogram of  $\text{ZnFe}_2\text{O}_4$  (ZF-1) calcined at  $500^\circ\text{C}$ .

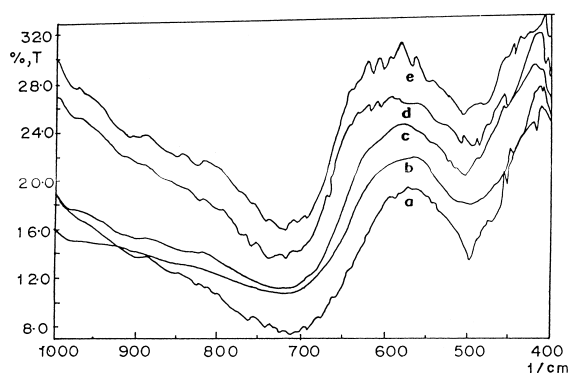


Fig. 2. Diffuse reflectance infrared spectra of different Zn–Ni ferrite systems: (a) ZF-1; (b) ZNF-2; (c) ZNF-3; (d) ZNF-4; (e) NF-5.

[22] and by White and DeAngelis [23] that the high frequency band at  $700\text{ cm}^{-1}$  is due to the stretching vibration of the tetrahedral group and the lower frequency band at  $500\text{ cm}^{-1}$  is due to the vibration of the octahedral M–O group. According to Waldren [22], the tetrahedral bonds have the effect of substantially increasing the frequency for vibration, since these cations introduce a supplementary restoring force in a preferential direction along the  $M_{T-O}$  bond. The BET surface areas of the different compositions of the ferrite systems were determined using an OMNISORP 100 CX instrument; the results are presented in Table 1.

### 2.2.2. Surface properties – acidity/basicity

Two independent methods were adopted to evaluate the acidity and basicity of the systems. Dehydration activity of the systems can be correlated with their surface acidity. In the present case one such experi-

Table 2

Cyclohexanol dehydration activity and the limiting values of electron acceptors (EA) adsorbed over different Zn–Ni ferrite systems

Catalyst composition	Cyclohexene <sup>a</sup> (%)	Limiting amount of EA adsorbed ( $\times 10^{-5}\text{ mol/m}^2$ )	
		TCNQ	Chloranil
ZF-1	39.72	1.561	0.658
ZNF-2	35.28	1.763	0.730
ZNF-3	29.57	1.910	0.836
ZNF-4	19.17	2.192	1.020
NF-5	12.03	2.382	1.060

<sup>a</sup> Reaction conditions: catalyst amount 3 g; flow rate 4 ml/h; temperature  $325^\circ\text{C}$ .

ment using cyclohexanol as the substrate has been performed. The reaction is carried out in a down-flow vapor phase silica reactor. The detailed reaction procedure is given elsewhere [24]. Mol% of cyclohexene formed has been taken as the direct measure of the acidity of the system (Table 2).

For the determination of the basicity of the system, adsorption studies of electron acceptors (EA) were performed. The utility of electron acceptor adsorption for the study of the electron donor properties of the surface has been well established [25–29]. 7,7,8,8-tetracyanoquinodimethane (TCNQ), 2,3,5,6-tetrachloro-1,4-benzoquinone (chloranil) and *p*-dinitrobenzene (PDNB) with electron affinity values 2.84, 2.40 and 1.77 eV, respectively, were employed for this study. Catalysts were activated at  $500^\circ\text{C}$  prior to each experiment. The adsorption study was carried out over 0.5 g catalyst placed in a cylindrical glass vessel fitted with an air-tight stirrer. A solution of EA in acetonitrile

Table 1

Physico-chemical characteristics of Zn–Ni ferrite systems

Composition (x)	Cation at		Concentration <sup>a</sup> (%)		Surface area <sup>b</sup> ( $\text{m}^2/\text{g}$ )
	T-site	O-site	Zn <sup>2+</sup>	Ni <sup>2+</sup>	
0	Zn <sup>2+</sup>	Fe <sup>3+</sup>	27.0 (27.1)	–	30.0
0.2	Zn <sub>0.8</sub> <sup>2+</sup> Fe <sub>0.2</sub> <sup>3+</sup>	Ni <sub>0.2</sub> <sup>2+</sup> Fe <sub>1.8</sub> <sup>3+</sup>	21.6 (21.8)	4.9 (4.9)	30.3
0.5	Zn <sub>0.5</sub> <sup>2+</sup> Fe <sub>0.5</sub> <sup>3+</sup>	Ni <sub>0.5</sub> <sup>2+</sup> Fe <sub>1.5</sub> <sup>3+</sup>	13.7 (13.8)	12.3 (12.3)	47.6
0.8	Zn <sub>0.2</sub> <sup>2+</sup> Fe <sub>0.8</sub> <sup>3+</sup>	Ni <sub>0.8</sub> <sup>2+</sup> Fe <sub>1.2</sub> <sup>3+</sup>	5.4 (5.6)	20.0 (20.0)	57.7
1.0	Fe <sup>3+</sup>	Ni <sup>2+</sup> Fe <sup>3+</sup>	–	24.9 (25.0)	60.9

<sup>a</sup> Quantities in the parentheses indicate the theoretical value.

<sup>b</sup> Specific surface area of samples calcined at  $500^\circ\text{C}$ .

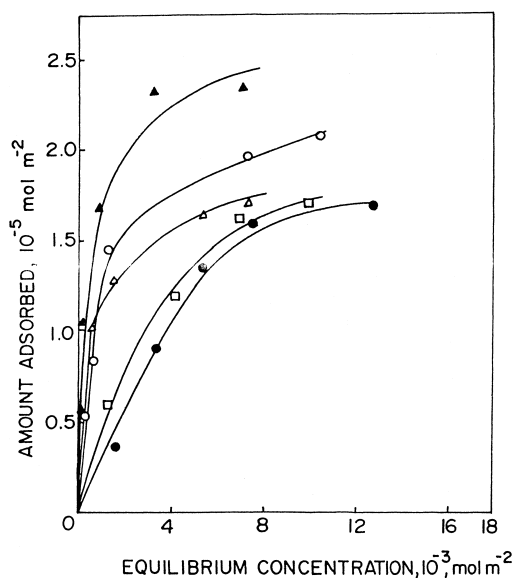


Fig. 3. Adsorption isotherms of TCNQ in acetonitrile on different Zn–Ni ferrite systems calcined at 500°C: (●) ZF-1; (□) ZNF-2; (△) ZNF-3; (○) ZNF-4; (▲) NF-5.

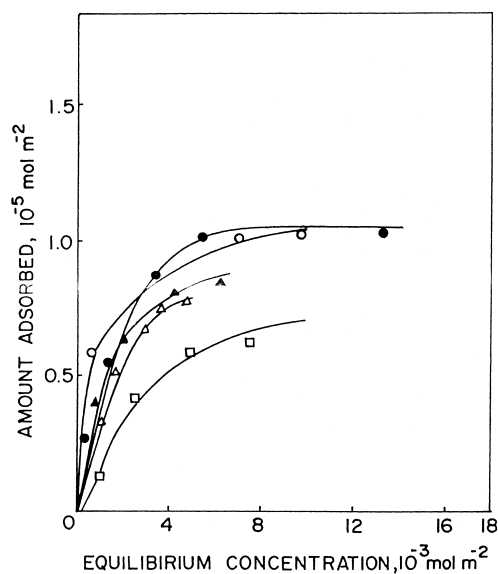


Fig. 4. Adsorption isotherms of chloranil in acetonitrile on different Zn–Ni ferrite systems calcined at 500°C: (□) ZF-1; (△) ZNF-2; (▲) ZNF-3; (○) ZNF-4; (●) NF-5.

trile was then admitted to the catalyst. Stirring was continued for 4 h at room temperature. The amount of EA adsorbed was determined from the difference in the concentration of EA in solution before and after adsorption, which was measured by means of a UV–VIS spectrophotometer ( $\lambda_{\max}$  of EA in solvent: 393.5 nm for TCNQ, 288 nm for chloranil and 262 nm for PDNB).

The limiting amounts adsorbed for TCNQ and chloranil are presented in Table 2. The adsorption of PDNB was negligible. Langmuir type adsorption isotherms obtained for TCNQ and chloranil are shown in Figs. 3 and 4, respectively. A strong electron acceptor (TCNQ) can accept electrons from both strong and weak donor sites, whereas weak EA (PDNB) can accept electrons from strong donor sites only. Negligible adsorption of PDNB in all systems indicates the absence of strong basic sites, and hence the limiting amount of TCNQ and chloranil would be an estimate of the weak or moderate basic sites. A survey of the limiting amount adsorbed (Table 2) indicates that basicity of the system follows the order: NF-5 > ZNF-4 > ZNF-3 > ZNF-2 > ZF-1, which indicates that basicity shows an increasing trend with progressive substitution of zinc by nickel. The increase in

basicity is associated with a concomitant decrease in their acidity, as revealed from the dehydration activity. From these results, it can be inferred that basic sites are created by  $\text{Ni}^{2+}$  ions and that either  $\text{Zn}^{2+}$  or  $\text{Fe}^{3+}$  ions are responsible for the acidity of the systems. Due to the  $d^{10}$  configuration of the  $\text{Zn}^{2+}$  ions and also due to their occupancy in the less accessible T-sites, we believe that the high strength Lewis acidity is created by the octahedral  $\text{Fe}^{3+}$  ions. A similar conclusion regarding acidity was reported by Dixit and co-workers [30] for Cu–Cr–Fe ternary spinel systems, since they observed a progressive decrease in the activation energy for Friedel–Crafts benzylation reaction as the iron content of the system increases.

### 3. Catalytic reactivity

#### 3.1. Apparatus and procedure

The alkylation experiments were carried out in a fixed-bed down-flow silica reactor (20 mm ID) at atmospheric pressure. The catalyst was placed at the center of the reactor; it was activated at 500°C in flowing air, and then brought down to the corre-

sponding reaction temperatures by cooling under a current of nitrogen gas of high purity. The mixture of aniline and methanol was fed by an ISCO-Model 500 D syringe pump. Liquid products were condensed with a cold trap and were analyzed by a Shimadzu GC-15 A gas chromatograph using FID and 2 M, 2% carbowax 20 M+5% KOH on a chromosorb W column. The gaseous products were analyzed using a porapak-Q column with TCD. A blank run without any catalyst indicated negligible thermal reaction.

### 3.2. Results and discussion

Methylation of aniline is a multistep sequential reaction; the main reaction scheme of which can be represented as follows:

Aniline + MeOH  $\rightarrow$  *N*-methyl aniline(NMA) and/or toluidines

NMA + MeOH  $\rightarrow$  *N,N*-dimethyl aniline(NNDMA) and/or *N*-methyl toluidines

NNDMA + Aniline  $\rightarrow$  2NMA

### Toluidines + MeOH $\rightarrow$ Xylidines

Among the various compositions of the system ( $Zn_{1-x}Ni_xFe_2O_4$ ), the systems with “*x*” values 0, 0.2 and 0.5 were found to be selective for mono *N*-alkylation, even though catalytic activity showed a significant gradation with their “*x*” values. However, systems possessing the highest “*x*” values were found to be less active for this reaction, probably due to the highest methanol decomposition rate over the nickel-containing systems. Even in the most active catalyst ( $x=0$ ), the percentage of *C*-alkylated product was found to be less than 0.2% under the optimized reaction conditions.

Fig. 5 shows the influence of molar ratio of the reactants on the activity over ZF-1. With all the catalyst systems, NMA has been detected as the major product. Both NMA yield and aniline conversion increased with (methanol to aniline) molar ratio and at the molar ratio 7, the yield of NMA was maximized (67.1%). Highest amount of NNDMA (3.9%) has also been detected at this stage. This result clearly indicates that the increase in methanol to aniline molar ratio does not significantly increase the *N,N*-dialkylation

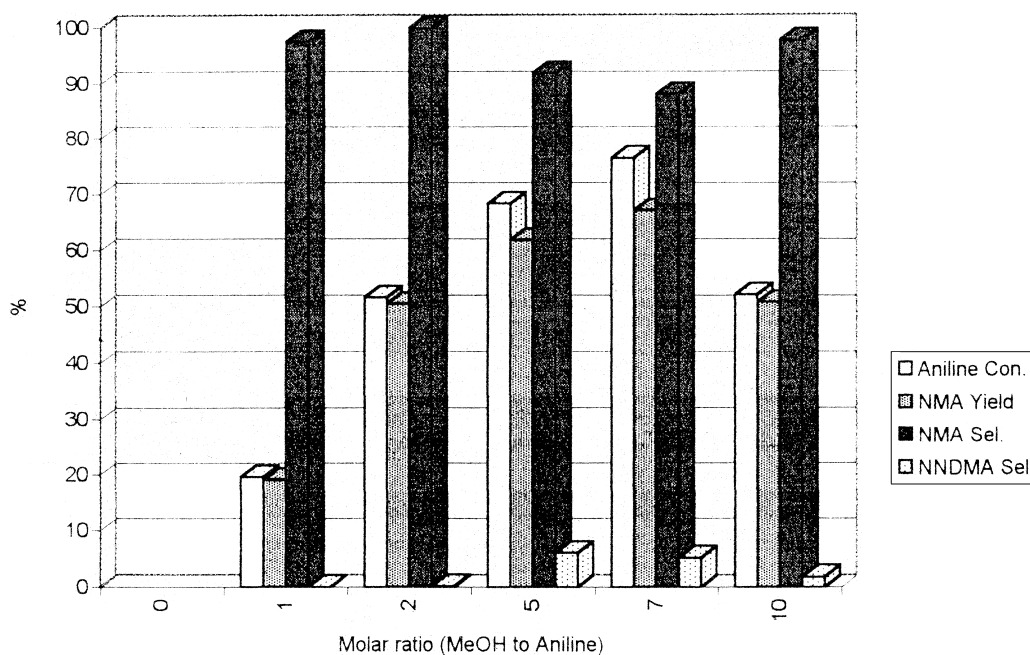


Fig. 5. Influence of feed (methanol to aniline) molar ratio on conversion and selectivities. Catalyst ZF-1; WHSV  $2 \text{ h}^{-1}$ ; reaction temperature 623 K; TOS 1 h.

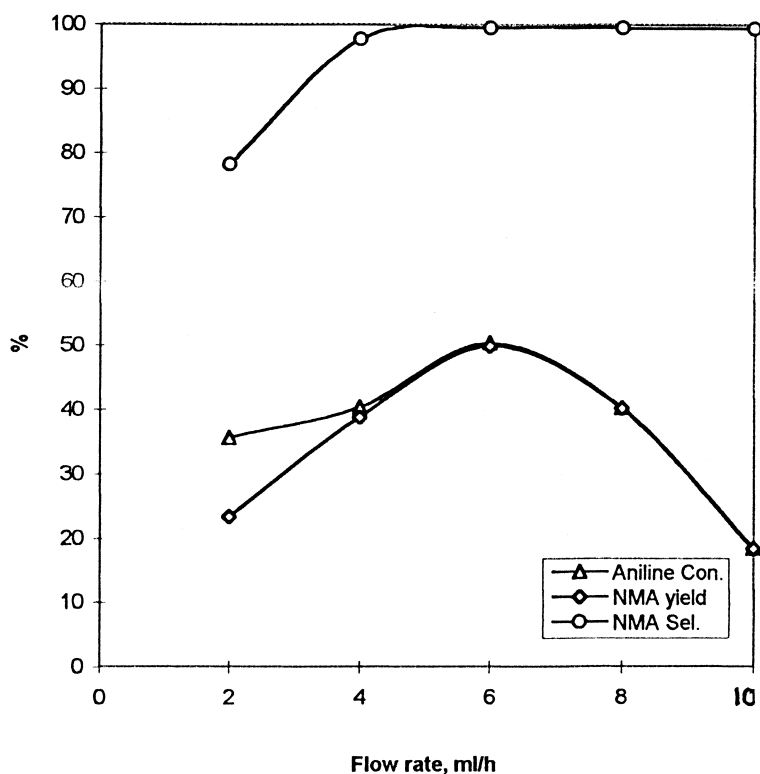


Fig. 6. Effect of feed flow rate on NMA selectivity, yield and aniline conversion over ZF-1. Catalyst amount 3 g; molar ratio (methanol to aniline) 2; reaction temperature 623 K; TOS 1 h.

rate and thereby decrease NMA selectivity. Interestingly, about 50.5% NMA was formed even at a feed mix ratio of 2 with selectivity more than 99.7%.

In another series of experiments, the effect of contact time on the activity was studied. A typical activity profile of aniline methylation as a function of feed rate (WHSV varies from 0.67 to 3.3 h<sup>-1</sup>) over ZF-1 is shown in Fig. 6. The yield of NMA was maximized at the flow rate 6 ml/h (WHSV, 2 h<sup>-1</sup>). The selectivity of NMA was found to be about 99.5% at this stage. But, as shown in the figure, aniline conversion reached a maximum and then decreased by increasing flow rate. The low aniline conversion rate at high contact time region can be attributed to the increased rate of methanol decomposition as a side reaction. Since the methanol to aniline molar ratio is only 2, such side reaction of methanol will seriously affect aniline conversion. As contact time decreases, the rate of this side reaction also decreases, resulting in more aniline conversion and NMA yield.

The alkylation experiments were performed in the temperature range 300–400°C over ZF-1. Table 3 shows the influence of temperature on the product distribution. Optimum temperature for maximum NMA yield and aniline conversion was at 340–350°C. As is evident from the table, there was a slight enhancement in the selectivity of NNDMA as temperature was increased from 300°C to 400°C. However, beyond 350°C the aniline conversion was declined and lesser amount of NMA was formed. MeOH decomposition rate seemed to enhance at this stage, since the analysis of the gaseous products indicates the presence of considerable amount of formaldehyde and C<sub>1</sub> and C<sub>2</sub> hydrocarbons.

Another set of experiments were carried out to establish the stability of the systems. In Fig. 7 the yield of NMA is plotted as a function of time-on-stream (TOS). All catalysts except ZF-1 displayed excellent stability even after 10 h. ZF-1 showed deactivation in the initial period of the run (up to 4 h) and

Table 3  
Performance of ZF-1 for aniline methylation at different reaction temperatures

	Reaction temperature		
	300°C	350°C	400°C
Aniline conversion (wt%)	55.96	71.46	57.71
Product distribution (wt%)			
Benzene	Nil	0.24	1.25
Toluene	0.73	1.04	1.75
NMA	54.30	67.1	50.95
NNDMA	0.75	3.90	3.15
Toluidines	Nil	Nil	0.15
Others	0.16	0.2	0.40
Product selectivity (wt%)			
NMA	97.03	93.90	88.37
NNDMA	1.34	5.40	5.45

WHSV, 2 h<sup>-1</sup>; methanol to aniline molar ratio 7; TOS 1 h.

thereafter it maintained a steady value of activity. This result is particularly interesting if one considers the

normal spinel lattice of ZF-1, where electron hopping is constrained due to the non-availability of Fe<sup>3+</sup> ions in the T-sites. Others are inverse in nature and all such systems showed prolonged stability.

The effect of catalyst composition on activity and selectivity is shown in Fig. 8. Catalytic activity follows the order: ZF-1>ZNF-2>ZNF-3>ZNF-4>NF-5. Since acidity values of the systems were also found to follow the same order, the gradation in activity can be explained by considering factors like variation of acidity with Ni<sup>2+</sup> substitution and its direct influence on the distribution of active Fe<sup>3+</sup> ions in the spinel lattice.

The mechanism of the aniline alkylation reaction was well established by Nan Ko et al. [31], according to which Lewis acid sites of the metal oxide systems interact with the methoxy species, and the hydrogen atoms of the undissociated hydroxyl groups interact with the Lewis basic sites (Fig. 9). Electrophilic attack of the methyl group of the methanol on the nitrogen

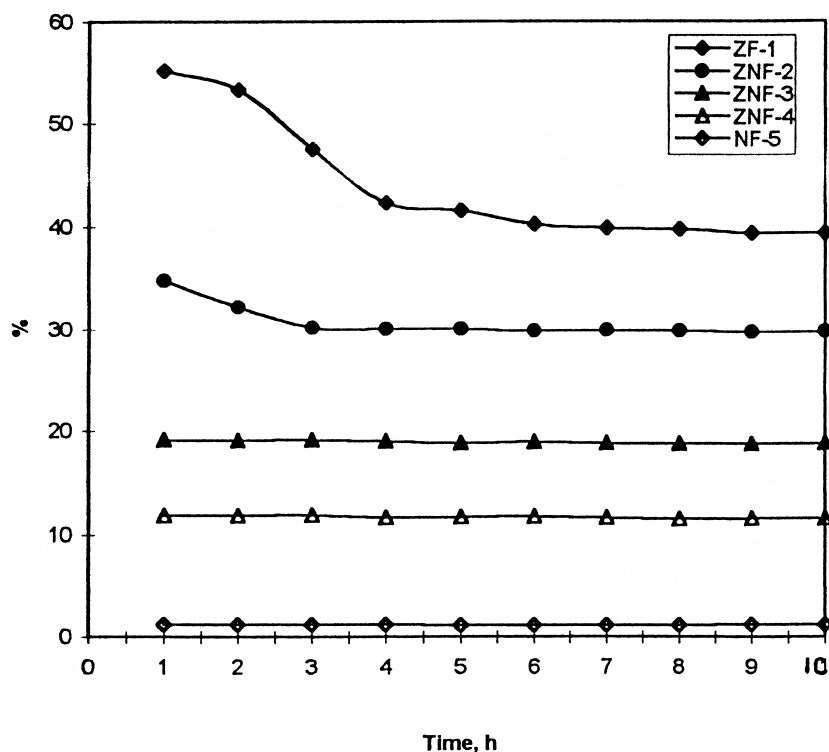


Fig. 7. Effect of time-on-stream: WHSV 1.3 h<sup>-1</sup>; reaction temperature 623 K; methanol to aniline molar ratio 2. Concentration of *N*-methyl aniline is plotted as a function of reaction time in hours.

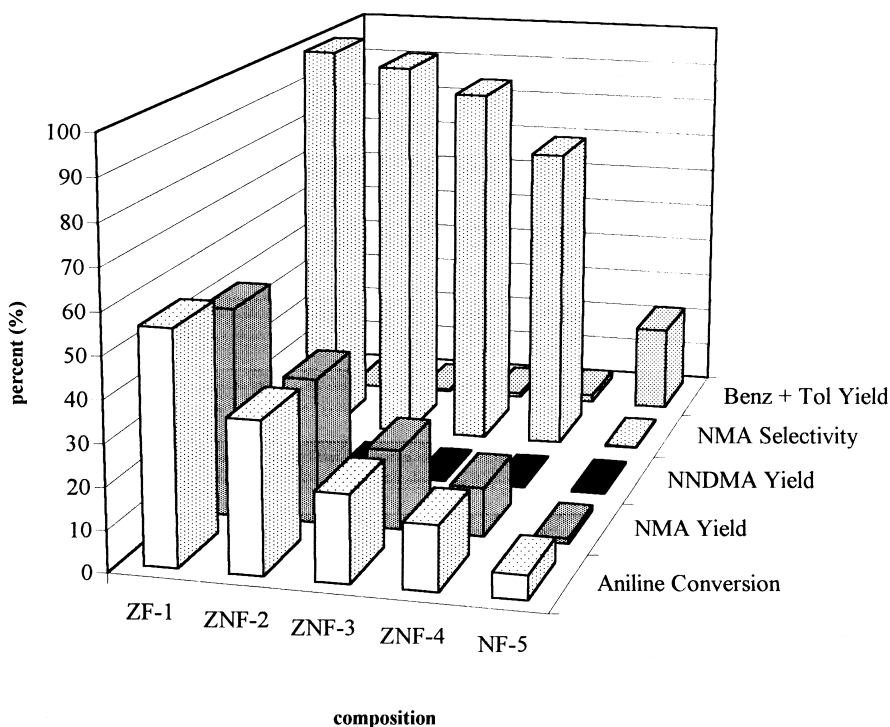


Fig. 8. Product distribution and selectivity pattern of aniline alkylation over different Zn–Ni ferrite systems. Reaction temperature 623 K; WHSV  $2 \text{ h}^{-1}$ ; methanol to aniline molar ratio 2:1; TOS 1 h.

atom of the adsorbed aniline leads to NMA, which on subsequent methylation leads to NNDMA. Thus the mechanism accounts for the need of moderate amounts of both acidic and basic Lewis sites for the system. However, this mechanism differs from the one suggested by Rao and co-workers [32] for ALPO and SAPO, since in the latter case adsorption and subsequent polarization of the substrates is mainly caused by Brønsted acidity on the surface. Any factor that alters either acidity or basicity of the present system will significantly influence the selectivity of the products and the activity of the system.

From the adsorption study of EAs and their dehydration activity, it is clear that substitution of  $\text{Zn}^{2+}$  by  $\text{Ni}^{2+}$  creates a decrease in acidity with a concomitant increase in basicity. Both acidity and catalytic activity of the systems follow the order: ZF-1 > ZNF-2 > ZNF-3 > ZNF-4 > NF-5. The high strength Lewis acidity can probably be due to the  $\text{Fe}^{3+}$  ions in the O-sites because of the stable nature of  $\text{Zn}^{2+}$  ions ( $d^{10}$  configuration) and also due to their occupancy in the less accessible

T-sites. As “ $x$ ” increases,  $\text{Ni}^{2+}$  ions replace  $\text{Fe}^{3+}$  ions isomorphically from O-sites to T-sites, leading to decreases in the activity of the systems. In other words, the low activity can be accounted for as due to the replacement of acidic sites by basic sites during  $\text{Ni}^{2+}$  substitution. This is clearly evidenced from the adsorption study of EAs, since  $\text{Ni}^{2+}$  substitution progressively increased the limiting concentration of EAs adsorbed (Figs. 3 and 4). Since aniline is a strong base, even weak Lewis sites can also effectively co-ordinate with this molecule, and therefore, the liability of the systems towards alcohol adsorption becomes more important. It was reported that the lower valency and coordination number of T-ions lead to a strong M–O interaction [7,33]. In ferrites, the  $\text{Fe}^{3+}$ –O distance is more when  $\text{Fe}^{3+}$  is in octahedral symmetry than in the tetrahedral symmetry. Hence, such  $\text{Fe}^{3+}$  ions will be readily available for adsorption of alcohol. From these, it is clear that  $\text{Fe}^{3+}$  ions in the O-sites are mainly responsible for the activity of the system.



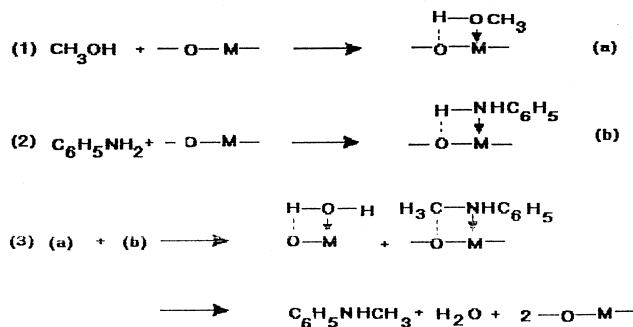
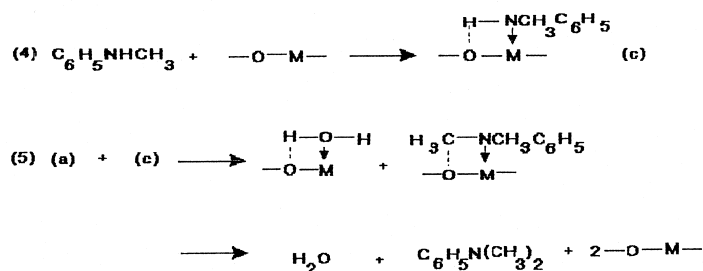
Mechanism of N-monomethylation:Mechanism of N,N-dimethylation:

Fig. 9. Mechanism of N-methylation of aniline.

The stability of the systems can also be explained by considering the above-mentioned structural features of the systems and the ease with which such systems can undergo oxidative migration after alcohol adsorption. Adsorption of alcohol leads to electron transfer from adsorbate to catalyst, which changes the oxidation state of iron. However, if  $\text{Fe}^{3+}$  ions are available in the neighboring T-sites, reduced  $\text{Fe}^{3+}$  ions can regain their original state by electron exchange. ZF-1 being a normal spinel, these types of electron exchanges are not possible and hence in the reducing atmosphere such systems deactivate at a faster rate than the corresponding inverse systems.

#### 4. Conclusion

1.  $\text{Zn}_{1-x}\text{Ni}_x\text{Fe}_2\text{O}_4$  ( $x=0, 0.2, 0.5, 0.8$  and  $1$ ) type systems were studied for alkylation of aniline using methanol as the alkylating agent. It was

observed that these systems (except the one possessing “ $x$ ”=1) can effectively alkylate aniline to give *N*-methyl aniline selectively. More than 99% NMA selectivity was observed under the optimized reaction conditions. Even at low concentration of methanol in the feed, these systems exhibited high activity.

2. Activity decreases as “ $x$ ” increases. Highest activity was observed for ZF-1, whereas NF-5 was only mildly active.
3. As “ $x$ ” increases, the basicity of the system also increases.  $\text{Ni}^{2+}$  ions isomorphically replace acidic  $\text{Fe}^{3+}$  ions from the active O-sites to T-sites, leading to a progressive diminishing in the activity.
4. ZF-1 is a normal spinel system. As “ $x$ ” increases, the system progressively approaches to an inverse lattice. All inverse systems (i.e., other than “ $x$ ”=0) displayed prolonged stability. This is due to the possibility of the redox migration among the Fe ions in the O- and the neighboring T-sites. Non-

availability of Fe<sup>3+</sup> ions in the T-sites of ZF-1 causes deactivation, since the reduced Fe<sup>3+</sup> ions in the O-sites are unable to exchange electrons and thereby regain their original states.

## Acknowledgements

K.S thanks Dr. Paul Ratnasamy, Director, NCL, for providing facilities and CSIR, New Delhi, for a junior research fellowship.

## References

- [1] H.K. Harold, C.K. Mayfair, *Adv. Catal.* 33 (1985) 159.
- [2] R.R. Rajaram, A. Sermon, *J. Chem. Soc., Faraday Trans. 1* 81 (1985) 2577.
- [3] H.M. Cota, J. Katan, M. Chin, F.J. Schoenweis, *Nature (London)* 203 (1964) 1281.
- [4] J.R. Goldstein, A.C.C. Tseung, *J. Catal.* 32 (1974) 452.
- [5] G.R. Dube, V.S. Darshane, *Bull. Chem. Soc. Jpn.* 64 (1991) 2449.
- [6] T. Takada, Y. Bando, M. Kiyama, T. Shinjo, in: Y. Hoshino, S. Iida, M. Suginoo (Eds.), *Proceedings of the International Conference on Ferrites, Japan, July 1970*, University of Tokyo Press, Japan, 1971, pp. 29–31.
- [7] F.C. Romeijn, *Phil. Res. Rep.* 8 (1953) 304.
- [8] J.P. Jacobs, A. Maltha, J.R.H. Reintjes, T. Drimal, V. Ponec, H.H. Brogersma, *J. Catal.* 147 (1994) 294.
- [9] S. Narayanan, V. Durgakumari, A.S. Rao, *Appl. Catal. A* 111 (1994) 133.
- [10] J. Santhanalakshmi, T. Raja, *Appl. Catal. A* 147 (1996) 69.
- [11] O. Onaka, K. Ishikawa, Y. Isumi, *Chem. Lett.* (1982) 1783.
- [12] W.W. Kaeding, R.E. Holland, *J. Catal.* 109 (1988) 212.
- [13] S. Prasad, B.S. Rao, *J. Mol. Catal.* 62 (1990) L17.
- [14] A. Nanko, C.L. Yang, W. Zhu, H. enLin, *Appl. Catal. A* 134 (1996) 53.
- [15] F.M. Bautista, J.M. Campelo, A. Garcla, D. Luna, J.M. Marriars, A.A. Romero, *Appl. Catal. A* 166 (1998) 39.
- [16] F.M. Bautista, J.M. Campelo, A. Garcla, D. Luna, J.M. Marriars, A.A. Romero, M.R. Urbano, *J. Catal.* 172 (1997) 103.
- [17] C.M. Naccache, Y.B. Tarit, *J. Catal.* 22 (1971) 171.
- [18] A.N. Ko, C.L. Yang, W. Zhu, H. Lin, *Appl. Catal. A* 134 (1996) 53.
- [19] A.G. Hill, J.H. Ship, A.J. Hill, *Ind. Eng. Chem.* 43 (1951) 1579.
- [20] H. Matsushashi, K. Arata, *Bull. Chem. Soc. Jpn.* 64 (1991) 2605.
- [21] P.S. Anilkumar, J.J. Schotri, S.D. Kulkarni, C.E. Deshpande, S.K. Date, *Mat. Lett.* 27 (1996) 293.
- [22] R.D. Waldren, *Phys. Rev.* 99 (1955) 1727.
- [23] W.B. White, B.A. DeAngelies, *Spectrochim. Acta, A* 23 (1967) 985.
- [24] W.S. Chin, M.D. Lee, *Appl. Catal. A* 83 (1992) 201.
- [25] K. Isumi, K. Meguro, *J. Adhesion Sci. Technol.* 4 (1990) 393.
- [26] S. Sugunan, G.D. Rani, *J. Mat. Sci. Lett.* 10 (1991) 887.
- [27] H.P. Leftin, M.C. Hobson, *Adv. Catal.* 14 (1963) 163.
- [28] A. Terinin, *Adv. Catal.* 15 (1964) 256.
- [29] R.P. Porter, W.K. Hall, *J. Catal.* 5 (1966) 366.
- [30] S.P. Ghorpade, V.S. Darshane, S.G. Dixit, *Appl. Catal. A* 166 (1998) 141.
- [31] A.N. Ko, C.L. Yang, W. Zhu, H. enLin, *Appl. Catal.* 134 (1996) 53.
- [32] P.S. Singh, R. Bandyopadhyay, B.S. Rao, *Appl. Catal. A* 136 (1996) 177.
- [33] C.S. Narasimhan, C.S. Swami, *Appl. Catal.* 2 (1982) 315.